

Nanocomposite Titania–Carbon Spheres as CO₂ and CH₄ Sorbents

Antoni W. Morawski, Piotr Staciwa, Daniel Sibera, Dariusz Moszyński, Michał Zgrzebnicki, and Urszula Narkiewicz*



Cite This: <https://dx.doi.org/10.1021/acsomega.9b03806>



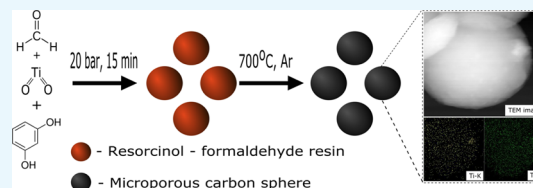
Read Online

ACCESS |

Metrics & More

Article Recommendations

ABSTRACT: Photocatalysis can offer solutions for the transformation of greenhouse gases, such as methane and carbon dioxide. In the paper, a candidate for such a photocatalyst is presented, based on a composite of titania with carbon spheres. The material was obtained using microwave assisted solvothermal synthesis, enabling good dispersion of titania. The studies of carbon dioxide and methane adsorption were performed under ambient pressure and temperatures of 40, 60, and 80 °C. The effect of temperature increase was less favorable for carbon dioxide than for methane. Satisfying values of carbon dioxide and methane uptake were obtained—3.94 mmol CO₂/g and 2.77 mmol CH₄/g at 40 °C.



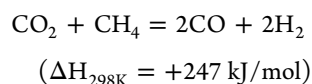
1. INTRODUCTION

Global warming observed recently and causing severe weather phenomena is mainly due to the emission of greenhouse gases. The task of reducing greenhouse gas emissions, especially carbon dioxide and methane, poses a great challenge because of their abundance.

At present, the separation and storage of both gases is performed, whereas their utilization still needs new approaches and further studies.

Although both carbon dioxide and methane have a negative impact on climate change, the global warming potential of methane is almost 25 times higher than that of carbon dioxide.¹

An ideal solution would be to combine both greenhouse gases, carbon dioxide and methane, in a reaction leading to some useful products, for example, syngas, according to the reaction



Although the thermodynamics of the reaction is not favorable, the issue of process feasibility should be addressed. Catalytic dry reforming was intensively investigated at the end of the 20th century² and several processes were proposed to decrease the high thermodynamic barrier, such as plasma technologies, microwaves processes, solar thermal aerosol flow reactors, fixed bed reactors induced with electrical current, and electrochemical and photocatalytic processes.

Since the last option is the most environmentally friendly, the paper proposes a material, which can be applied as a successful photocatalyst in dry reforming of methane with carbon dioxide.

The effective photocatalytic reduction of CO₂ contains four main steps:³ CO₂ and CH₄ adsorption on the photocatalyst surface, electron–hole pair generation by adsorbing sufficient incident photon energy, electron–hole pair separation, and CO₂ reduction. Recent reports on photocatalytic dry reforming^{4–10} have focused on the performance of photocatalytic conversion, without deeper studies on the first-step adsorption of the reactants—CO₂ and CH₄. The adsorption of reactants is crucial because it increases contact of a reactant with the surface and enables its further transformation. Our paper, focusing on the adsorption of reactants on the photocatalyst surface, attempts to bridge the gap. A composite system based on microporous carbon spheres doped with titania was chosen and produced using a microwave-assisted hydrothermal method. Such composites are innovative and have not been reported in the literature up to now.

The research hypothesis was based on the fact that microporosity of carbon spheres should be favorable for both reactants' adsorption and micropores would play the role of microreactors in the next step—photocatalytic process. As titania is well known to be an efficient photocatalyst, decoration of carbon spheres with titania would be appropriate for future photocatalytic processes. Additionally, the positive impact of the synergy of both composite components on the photocatalyst performance can be expected. There are some recent literature reports about various modifications of titania materials applied for photocatalytic conversion of CO₂ and CH₄. Typical surface modifications are metal deposition, alkali

Received: November 8, 2019

Accepted: January 3, 2020

modification, carbon-based material loading, heterojunction construction, or impurity doping.³ A positive effect of the presence of Ti^{3+} sites and oxygen vacancies was reported,⁶ strongly enhancing visible-light absorption and decreasing band gap energy. It was mentioned by Low³ that the formation of Ti^{3+} sites on the surface was beneficial for binding of CO_2 and separation of electron and hole pairs. A significant presence of Ti^{3+} was confirmed by electron paramagnetic resonance with coefficient g_{eff} from 1.948 to 1.959 and oxygen vacancies.^{11,12}

According to the previous studies of our group, hybrid graphene (or graphene oxide) nanocomposites with TiO_2 may affect suppression of recombination or charge-carrier trapping. To investigate the phenomenon, we utilized the time resolve microwave conductivity method.¹³

In the present study, graphitic carbon spheres were prepared with oxygen groups on the surface, containing titania, as a future potential photocatalyst in dry reforming of methane. The idea is based on our preliminary positive results of the preparation of carbon spheres for CO_2 sorption.^{14,15}

Porous carbon materials are well known as efficient adsorbents of greenhouse gases because of their high surface area, microporosity, and mechanical and chemical stability. Their remarkable adsorption toward not only carbon dioxide^{16–18} but also methane^{19–21} has been widely investigated. Among porous carbon materials, carbon spheres provide uniform nanoscale shape of the material. The spherical shape of carbon materials can provide a better interface between the adsorbent and adsorbed material on the surface of the material. Additionally, carbon materials are open to modifications; thus, their extraordinary surface properties can be combined with the properties of other elements through doping carbon materials with functional elements such as N,^{22–24} Fe,^{25,26} and S.²⁷

TiO_2 is one of the most commonly known photocatalysts and offers inexpensive and sustainable (environmentally friendly) removal of water and air pollution. By combining porous carbon materials with TiO_2 , an efficient adsorbent with high photocatalytic activity can be obtained. There are many papers about preparation methods based on doping TiO_2 on the surface of commercial activated carbons^{28,29} or using the high energy-demanding chemical vapor deposition method and benzene as the carbon source.³⁰ Herein, we report a preparation method based on the low-temperature Stöber method, which allows us to tune the material physicochemical properties.^{14,31}

2. RESULTS AND DISCUSSION

2.1. Morphology. The morphology of pure carbon spheres and the produced composites was assessed using scanning electron microscopy (SEM). Their images are shown in Figure 1.

Comparing the images in Figure 1a,b, it can be stated that in both cases, very uniform carbon spheres were formed. Then, the addition of titania did not affect the morphology of the material. The mean diameter of the spheres increased following doping with titania. The average diameter of the obtained pure carbon spheres was about 570 nm, whereas that of the spheres with titania was about 800 nm (an increase of roughly 40%). The growth of diameter can be explained by an increasing number of crystallization nucleoli for the forming resin—the titania particles were the nucleation centers.

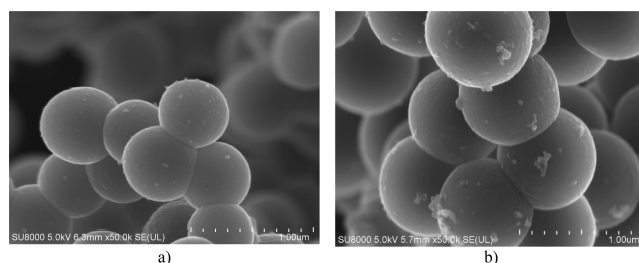


Figure 1. SEM images of pure carbon spheres [sample RF 700, (a)] and the composite of carbon spheres with titania [sample RF + Ti 700, (b)].

There are many literature reports about carbon–titania composites in which the surface of the carbon material is decorated with TiO_2 . The use of the Stöber method resulted in high dispersion of titania in the carbon matrix. It was proved using energy-dispersive X-ray (EDX) technique (Table 1),

Table 1. Quantitative Elemental Analysis by EDX

element	element wt (%)	atom (%)
C	77.4	87.2
O	11.3	9.6
Ti	11.3	3.2
total	100	100

showing a homogeneous distribution of titania nanoparticles in the whole volume of the material, within the assumed elemental composition. According to the mapping shown in Figure 2, a uniform distribution of all elements—carbon, oxygen, and titanium—can be observed.

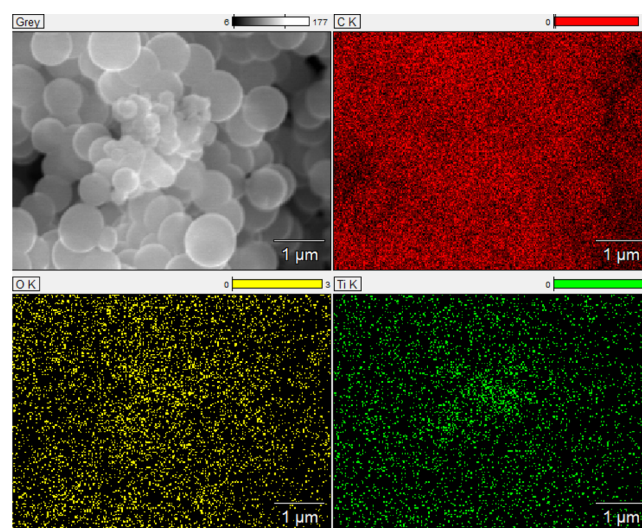


Figure 2. SEM image of carbon spheres doped with titania and EDX mapping of Ti, O, and C from TiO_2 –carbon spheres.

According to the transmission electron microscopy (TEM) studies, the diameter of spheres was similar to that observed in the SEM images (about 800 nm for the composite sample). At higher magnification (Figure 3a), neither typical carbonaceous structures nor titania crystallites could be observed. The image can correspond to a thin layer of titania on the surface of carbon spheres. The layer can be composed of amorphous titania or very small titania crystallites. For comparison, the

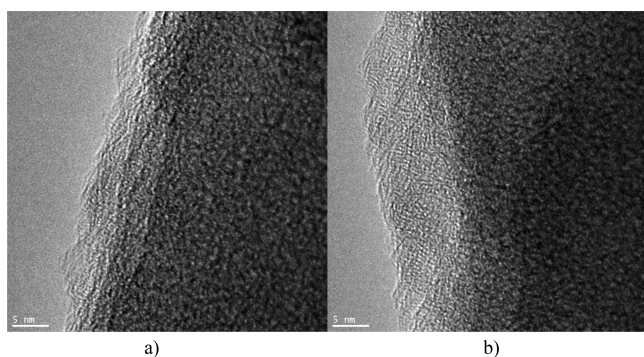


Figure 3. TEM image of carbon spheres doped with titania (a) and the image of pure carbon spheres (b).

TEM image of the pure carbon sample is shown in Figure 3b. Some multidomain disordered structures can be observed here. No typical graphite ordering can be seen.

The results of the mapping of the composite sample are shown in Figure 4. A sphere in the down right corner was

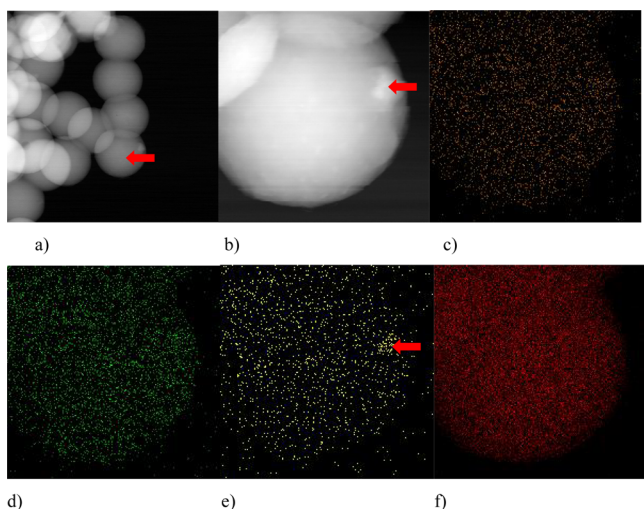


Figure 4. TEM images: (a,b), TEM mapping: (c) O–K, (d) Ti–L, (e) Ti–K, and (f) C–K.

analyzed (Figure 4a). A uniform distribution of the elements (O, Ti, and C) can be seen (Figure 4c–f). In the magnified image of the sphere (Figure 4b), an agglomeration of particles can be observed, marked with a red arrow. It corresponds to the agglomeration of titania particles, as can be concluded from titanium Ti–K mapping (Figure 4e).

2.2. X-ray Diffraction. The X-ray diffraction (XRD) pattern of the produced composite is shown in Figure 5. An increase in the background level in the area of low diffraction angles can be due to the presence of amorphous titania and/or carbon in the sample. The major peaks at 25.2, 37.8, 48, and 62.5° were assigned to the anatase phase of TiO₂.^{32,33} Only one peak at 27.5° can be ascribed to the rutile phase. Then, in the produced composite, the anatase phase was the dominating one, which is a big advantage in terms of photoactivity. Generally, the anatase phase (band gap \approx 3.2 eV) is more active than the rutile phase (band gap \approx 3.0 eV), but commercial photocatalysts contain both phases.^{34,35}

2.3. X-ray Photoelectron Spectroscopy. The quantitative evaluation of the surface of the RF + Ti 700 sample

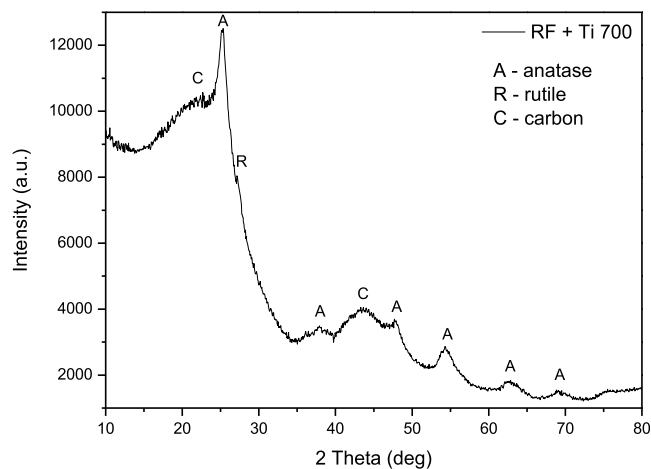


Figure 5. XRD diffractogram of the RF + Ti 700 sample.

indicates that carbon atoms constitute about 95% of all atoms detected by X-ray photoelectron spectroscopy (XPS) analysis (hydrogen was not observed). The rest consists of oxygen (3 at. %) and nitrogen (2 at. %). This result proves a high degree of carbonization of the sample. Titanium was not detected by XPS on the surface of the sample.

In Figure 6, an XPS spectrum of C 1s transition is presented. The maximum of the C 1s peak is located at 284.5 eV. The

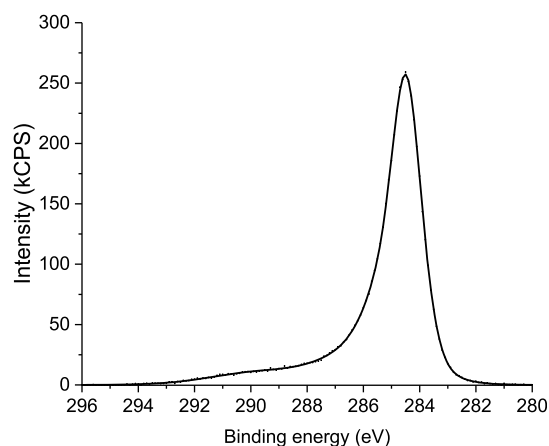


Figure 6. X-ray photoelectron spectrum of the C 1s region for the RF + Ti 700 sample.

maximum position is characteristic for elemental carbon but not for the pure graphite, which usually produces the XPS C 1s spectrum shifted toward lower binding energy (usually about 284.3 eV).³⁶ Therefore, it is supposed that carbon atoms form mainly sp³ bonds.

2.4. Specific Surface Area and Porosity. Nitrogen adsorption–desorption isotherms at -196 °C of pure carbon spheres and composite samples are presented in Figure 7. A higher volume of adsorbed nitrogen was observed for the pure carbon material; then, doping with titania caused some decrease in porosity. Both isotherms were a type I and type III mixture, typical for microporous solids.³⁷

The specific surface area was determined using the multipoint Brunauer–Emmett–Teller method with N₂ adsorption isotherms over a relative pressure (P/P_0). The total pore volume, including micropores and mesopores, was estimated by converting the amount of N₂ gas adsorbed at a

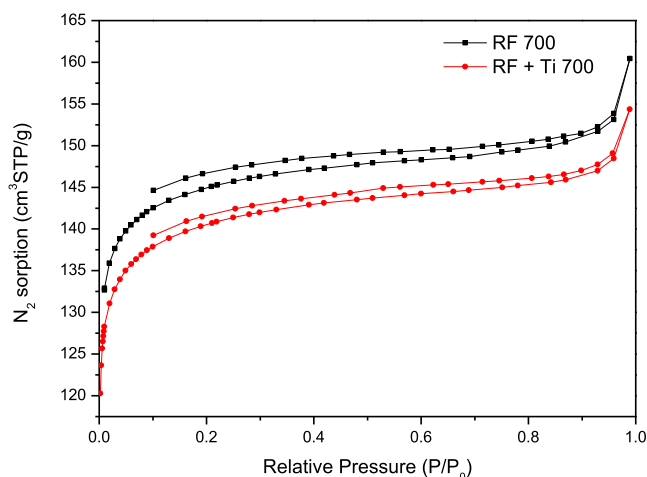


Figure 7. Adsorption–desorption isotherms of nitrogen at $-196\text{ }^{\circ}\text{C}$ for pure carbon and composite samples.

relative pressure of 0.9 to the liquid volume of the adsorbate (N_2). The micropore volume was determined using density functional theory. The results are shown in Table 2. The addition of titanium IV isopropylate caused a slight decrease in the specific surface area of the material. Nevertheless, the values of the total pore volume of both tested samples were similar.

Because low temperature nitrogen adsorption is effectively used mainly to determine mesopores above 2 nm, the obtained results should be treated only as an approximation, and the adsorption of carbon dioxide described in the next part of the paper will shed more light on the presence of micropores, thanks to the smaller kinetic diameter of the carbon dioxide molecule.

The adsorption capacity is a function of the surface area but also of the surface chemistry and microporosity of the material. For CO_2 adsorption, pores below 1 nm are the most important.³⁸ Figure 8 shows the pore size distribution of the obtained samples. In both cases, large peaks below 0.7 nm were detected. According to Yin et al.,³⁹ such a size of pores has significant influence on CO_2 uptake at 273.0–293.0 K at a P_{CO_2} of 0.01–0.10 MPa. Furthermore, Presser et al.⁴⁰ reported that pores below 0.8 nm are mainly responsible for CO_2 uptake at 273 K and 0.1 MPa. A significant weakening of the peak at 0.85 nm can be noticed for the sample containing TiO_2 . This observation is very important due to the role of micropores in adsorption of small gas molecules.

2.5. Greenhouse Gas Adsorption Studies. 2.5.1. Adsorption of Methane. The studies on adsorption of carbon dioxide and methane were performed on pure carbon spheres, on pure titania, and on the composite of titania–carbon spheres. The isotherms of adsorption–desorption of methane on these materials are presented in Figure 9 (carbon spheres) and Figure 10 (composite). The adsorption of methane on carbon spheres occurred (about three times) more efficiently than on titania (not shown here). The composite demon-

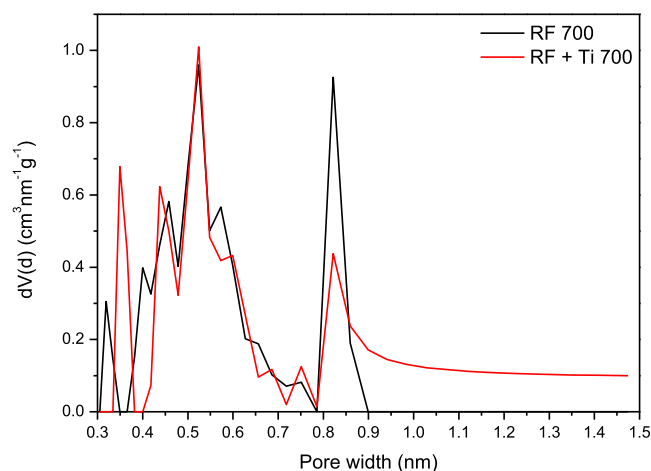


Figure 8. Pore size distribution of pure carbon and composite samples.

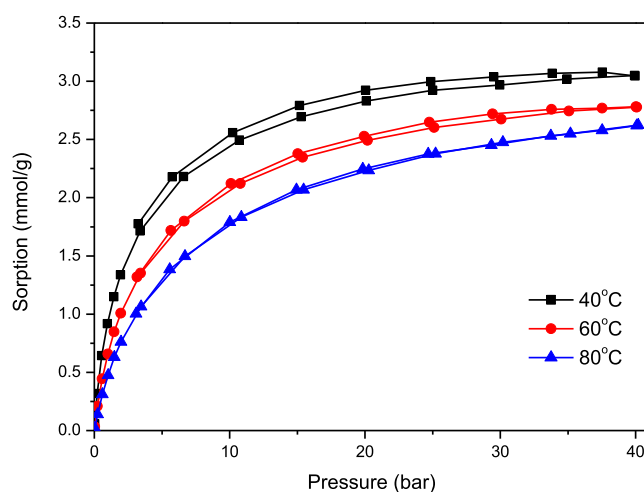


Figure 9. CH_4 adsorption–desorption isotherms on pure carbon spheres (sample RF 700).

strated similar (a little bit lower) adsorption capacity to pure carbon spheres. Some decrease of the adsorption capacity on the composite can be explained by the influence of titania addition as the yield of adsorbed methane on pure titania was much lower. However, some differences in behavior could be observed—in the case of the pure carbon material, there was almost no hysteresis at higher (60 and 80 $^{\circ}\text{C}$) temperature, so all adsorbed methane desorbed. In the case of titania and composite samples, a hysteresis could be observed (some volume of methane remained in the pores during desorption).

The optimistic conclusion from the results shown above can be that an increase in temperature caused only a weak decrease in the adsorption ability of methane, which is prospective for practical applications. The shape of the isotherms and the methane uptake level are similar for pure carbon spheres and the composite (higher methane uptake than pure titania). It

Table 2. Physicochemical Properties of the Samples

sample	S_{BET} (m^2/g)	total pore volume (cm^3/g)	micropore volume (cm^3/g)	density (g/cm^3)	CO_2 adsorption at 0 $^{\circ}\text{C}$, 1 at. (mmol/g)	CO_2 adsorption at 25 $^{\circ}\text{C}$, 1 at. (mmol/g)
RF 700	444	0.25	0.21	1.79	3.25	2.43
RF + Ti 700	432	0.24	0.20	1.83	3.19	2.03

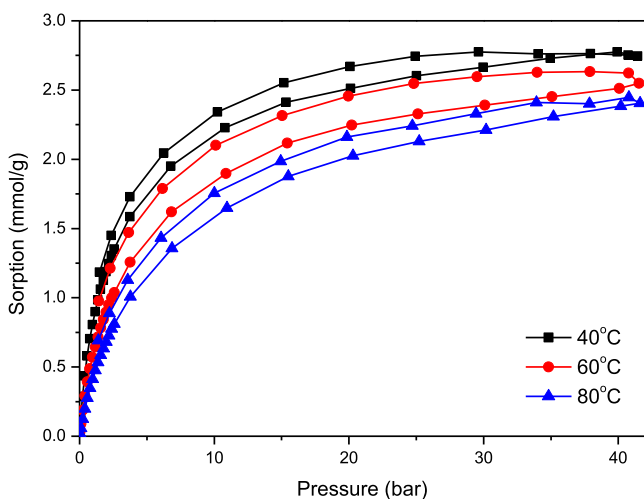


Figure 10. CH₄ adsorption–desorption isotherms on composite titania–carbon spheres.

can be then concluded that in the case of the titania–carbon sphere composite, adsorption of methane occurred mainly on carbonaceous structures.

2.5.2. Adsorption of Carbon Dioxide. To evaluate the rate of carbon dioxide adsorption on the produced composite, a kinetic test was performed using a thermogravimetric analyzer. The results are presented in Figure 11. The adsorption was fast as the steady state was reached after about 15 min only.

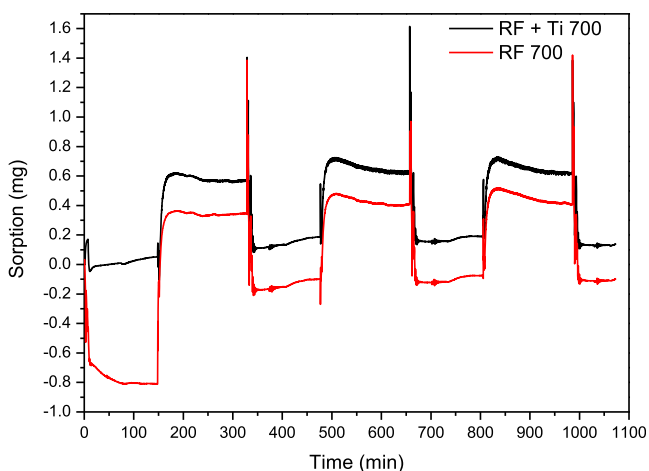


Figure 11. Thermogravimetric analysis curves for the CO₂ adsorption–desorption cycles.

The experimental results were kinetically presented by a pseudo-first-order kinetic model

$$\frac{da}{dt} = k(a^* - a)$$

where a^* and a (mmol/g) are the adsorption capacities at equilibrium and at time t , respectively, and k is the kinetic rate constant. After integration with boundary conditions $t = 0$ to $t = t$ and $a = 0$ to $a = a$, the following equations were obtained:

$$\ln \frac{a^* - a}{a^*} = -kt$$

$$a = a^*(1 - e^{-kt})$$

The results obtained using the pseudo-first-order kinetic model are shown in Table 3 and in Figure 12. The differences between the pure carbon and composite samples were negligible. A good correlation between experimental results and the model was obtained.

Table 3. Kinetic Model Parameters for CO₂ Uptake on the Presented Samples

sample	RF + Ti 700	RF 700
k [1/s]	0.243	0.245
R^2	0.956	0.985

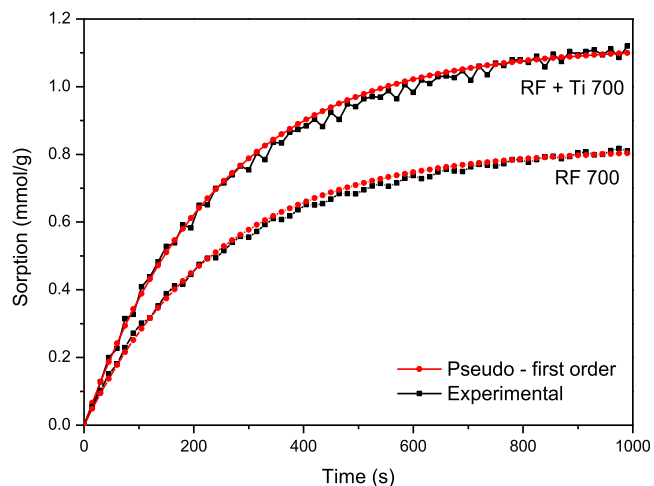


Figure 12. Experimental CO₂ uptake for the samples RF 700 and RF + Ti 700 and the corresponding fit to the kinetic model.

We have recently studied carbon dioxide adsorption on various types of titania. The adsorption capacity at ambient temperature was rather low, although an increase was observed after a surface treatment, which boosted its basicity. For crude titania,⁴⁰ the adsorption of CO₂ reached only 0.06 mmol CO₂/g at 30 °C, but after treatment of the material with NH₄OH and KOH, it increased ca. 9 times (to 0.53 mmol CO₂/g).⁴¹ The TiO₂/N material synthesized by hydrothermal reaction of amorphous anatase and NH₄OH at 100 °C was active in the photocatalytic reduction of chemisorbed carbon dioxide to methanol in a water solution.⁴² A similar behavior was observed for TiO₂ nanorods obtained from an alkali solution and modified with amines.⁴³ The modification with amines [tetraethylenepentamine (TEPA)] resulted in a considerable increase of CO₂ uptake in comparison with raw materials, that is, from 0.72 mmol CO₂/g to 3.02 mmol CO₂/g at 30 °C. The prepared samples were stable up to 150 °C and tested in multiple (6) adsorption–desorption cycles, without any performance deterioration. Interesting results were obtained from CO₂ adsorption on titanate–TiO₂ composites⁴⁴ modified with TEPA—in the range of 25–80 °C with increasing temperature, an increase of CO₂ uptake was observed from 2 mmol CO₂/g at 25 °C to 3.11 mmol CO₂/g at 80 °C. This unusual phenomenon indicates chemisorption of CO₂ on such materials, which is very promising for photocatalytic CO₂ reduction at the hole sites of TiO₂.

The results of CO₂ uptake measurements at 0 and 25 °C under atmospheric pressure on the samples produced within the study are presented in the last columns of Table 2. Doping of carbon spheres with titania caused a slight decrease in CO₂

uptake, from 3.25 to 3.19 at 0 °C and from 2.43 to 2.03 at 25 °C. The value of carbon dioxide uptake at 25 °C on the titania–carbon spheres composite was similar to that previously reported for titanate–TiO₂ composites.⁴⁴

It can be concluded that carbon dioxide adsorption occurred both on titania and carbon structures. It is a positive prognostic for the potential photocatalyst in which titania will contribute to the generation of electron–hole pairs and carbonaceous structures will suppress recombination or charge-carrier trapping.

Adsorption measurement results of carbon dioxide on pure carbon spheres and composite titania–carbon spheres at various temperatures are shown in Figures 13 and 14, respectively.

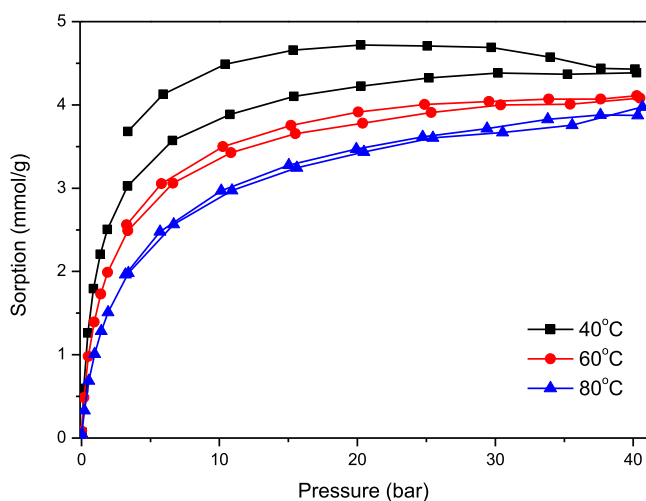


Figure 13. CO₂ adsorption–desorption isotherms on carbon spheres.

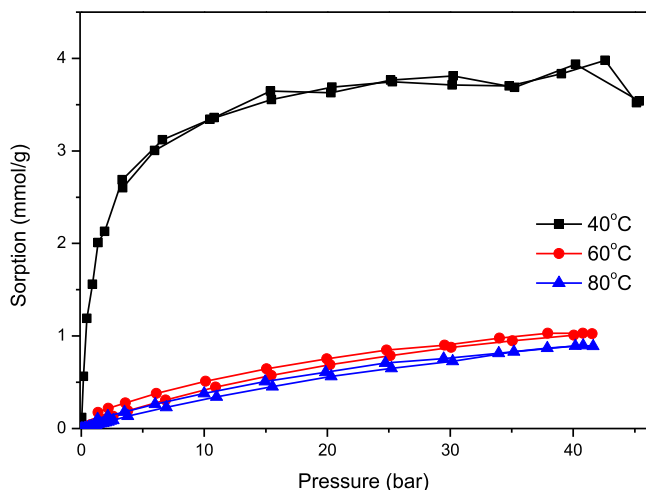


Figure 14. CO₂ adsorption–desorption isotherms on composite titania–carbon spheres.

Doping of carbon spheres with titania caused a decrease in carbon dioxide uptake, in particular, at higher temperature (60 and 80 °C). Nevertheless, doping with titania is recommended for further application of the material as a photocatalyst in dry reforming of methane with carbon dioxide. A temperature of 40 °C should be optimal for the efficient adsorption of both greenhouse gases.

3. MATERIALS AND METHODS

Preparation of the TiO₂–carbon composite was based on the Stöber method. The process was assisted by microwaves; thus the heat in the reaction volume was evenly distributed, which improved the quality of the obtained products. Resorcinol–formaldehyde resin was used as a carbon source. First, 0.6 g of resorcinol was dissolved in a mixture of 60 mL of distilled water and 24 mL of ethanol. Then, 0.19 mL of titanium IV isopropylate was added to the solution with continuous stirring in ambient conditions. The titanium–carbon weight ratio was 1:10. Afterward, 0.3 mL of ammonia and 0.9 mL of formaldehyde were added. The solution was stirred for 24 h and then transferred into an ERTEC MAGNUM II solvothermal microwave reactor at a pressure of 2 MPa for 15 min. Subsequently, the obtained mixture was dried at 80 °C for 2 days. The carbonization process was conducted in an argon atmosphere at 350 °C for 2 h at a heating rate of 1 °C/min and then, the temperature was raised to 700 °C with the same heating rate and the sample was kept at the final temperature for 2 h. Finally, the carbonized material was washed with distilled water and dried at 80 °C for 48 h. The composite sample was named “RF + Ti 700”, while the reference sample without titania was labeled “RF 700”.

The morphology of the produced samples was determined using a Hitachi SU8020 ultrahigh resolution field emission scanning electron microscope. TEM images were recorded using an FEI Tecnai F20 microscope.

The phase composition was determined using the XRD method. The phase composition of the prepared samples was studied with XRD using Cu K α radiation ($\lambda_{\text{Cu K}\alpha} = 0.1540$ nm) on an Empyrean, PANalytical. Identification of the crystalline phases was accomplished using HighScore+ software and the ICDD PDF-4+ 2015 database.

The chemical composition of the samples' surface was studied by XPS. The measurements were conducted using Mg K α ($h\nu = 1253.6$ eV) radiation in a Prevac (Poland) system equipped with a Scienta (Sweden) SES 2002 electron energy analyzer operating with constant transmission energy ($E_p = 50$ eV). The analysis chamber was evacuated to a pressure below 1×10^{-9} mbar. A powdered sample of the material was placed on a stainless steel sample holder.

To determine the textural properties of the carbon spheres, low temperature physical adsorption of nitrogen was carried out at –196 °C using a Quadrasorb volumetric apparatus (Quantachrome Instruments).

Carbon dioxide and methane adsorption isotherms were recorded at temperatures from ambient to 80 °C using a Sieverts IMI-HTP volumetric analyzer from Hiden Isochema Corporation.

The kinetics of carbon dioxide adsorption was studied using a thermogravimetric analyzer (Netzsch STA 449 C). The sample (9.92 mg) was placed in a sample pan and the temperature was raised from ambient to 30 °C, under the flow of nitrogen (30 mL/min) and then carbon dioxide (30 mL/min), until the steady state was reached. The same thermogravimetric apparatus was used to study thermal stability of the samples.

The choice of temperature range for adsorption measurements was driven by the future use of fabricated materials as sorbents of carbon dioxide from postcombustion hot gases. Deeper cooling of postcombustion gases would lead to a significant increase in costs of an industrial process and would

make the sorbents less attractive. Then, adsorption experiments of carbon dioxide and methane at ambient and above-ambient temperatures were conducted, even if the tests were much longer than those at lower temperatures.

Prior to each adsorption measurement, samples were degassed using vacuum at 250 °C for 16 h.

4. CONCLUSIONS

A new composite based on graphitic carbon spheres and titania was successfully synthesized using a microwave assisted solvothermal reactor. Good adsorption properties of the produced material toward methane and carbon dioxide predestine it to be used as a potential photocatalyst in dry reforming of these components, in which titania will contribute to the generation of electron–hole pairs and the role of carbonaceous structures would be also to diminish the recombination or charge-carrier trapping. Methane adsorption occurred mainly on carbon structures, while carbon dioxide was adsorbed both on titania and carbon sites. The optimum temperature for adsorption of both greenhouse gases on the titania–carbon sphere composite is about 40 °C. An open hysteresis loop indicated strong interaction of gases with the composite surface, contrary to the behavior of pure titania.

AUTHOR INFORMATION

Corresponding Author

Urszula Narkiewicz – West Pomeranian University of Technology in Szczecin, Szczecin, Poland; orcid.org/0000-0003-2443-1510; Email: urszula.narkiewicz@gmail.com

Other Authors

Antoni W. Morawski – West Pomeranian University of Technology in Szczecin, Szczecin, Poland

Piotr Staciwa – West Pomeranian University of Technology in Szczecin, Szczecin, Poland

Daniel Sibera – West Pomeranian University of Technology in Szczecin, Szczecin, Poland

Dariusz Moszyński – West Pomeranian University of Technology in Szczecin, Szczecin, Poland; orcid.org/0000-0002-7722-7540

Michał Zgrzebnicki – West Pomeranian University of Technology in Szczecin, Szczecin, Poland

Complete contact information is available at: <https://pubs.acs.org/10.1021/acsomega.9b03806>

Notes

The authors declare no competing financial interest.

ACKNOWLEDGMENTS

The authors acknowledge support from the National Science Centre with OPUS 17 grant 2019/33/B/ST8/02044.

REFERENCES

(1) Havran, V.; Duduković, M. P.; Lo, C. S. Conversion of methane and carbon dioxide to higher value products. *Ind. Eng. Chem. Res.* **2011**, *50*, 7089–7100.

(2) Lavoie, J.-M. Review on dry reforming of methane, a potentially more environmentally-friendly approach to the increasing natural gas exploitation. *Front. Chem.* **2014**, *2*, 1–17.

(3) Low, J.; Cheng, B.; Yu, J. Surface modification and enhanced photocatalytic CO₂ reduction performance of TiO₂: a review. *Appl. Surf. Sci.* **2017**, *392*, 658–686.

(4) Delavari, S.; Amin, N. A. S.; Ghaedi, M. Photocatalytic conversion and kinetic study of CO₂ and CH₄ over nitrogen-doped titania nanotube arrays. *J. Cleaner Prod.* **2016**, *111*, 143–154.

(5) Han, B.; Wei, W.; Chang, L.; Cheng, P.; Hu, Y. H. Efficient Visible Light Photocatalytic CO₂ Reforming of CH₄. *ACS Catal.* **2016**, *6*, 494–497.

(6) Wei, S.; Wu, R.; Jian, J.; Chen, F.; Sun, Y. Black and yellow anatase titania formed by (H,N)-doping: Strong visible-light absorption and enhanced visible-light photocatalysis. *Dalton Trans.* **2015**, *44*, 1534–1538.

(7) Liu, H.; Meng, X.; Dao, T. D.; Zhang, H.; Li, P.; Chang, K.; Wang, T.; Li, M.; Nagao, T.; Ye, J. Conversion of Carbon Dioxide T.D. by Methane Reforming under Visible-Light Irradiation: Surface-Plasmon-Mediated Nonpolar Molecule Activation. *Angew. Chem., Int. Ed.* **2015**, *54*, 11545–11549.

(8) Chung, W.-C.; Lee, Y.-E.; Chang, M.-B. Syngas production via plasma photocatalytic reforming of methane with carbon dioxide. *Int. J. Hydrogen Energy* **2019**, *44*, 19153–19161.

(9) Yazdanpour, N.; Sharifnia, S. Photocatalytic conversion of greenhouse gases (CO₂ and CH₄) using copper phthalocyanine modified TiO₂. *Sol. Energy Mater. Sol. Cells* **2013**, *118*, 1–8.

(10) Liu, L.; Zhao, C.; Xu, J.; Li, Y. Integrated CO₂ capture and photocatalytic conversion by a hybrid adsorbent/photocatalyst material. *Appl. Catal., B* **2015**, *179*, 489–499.

(11) Dolat, D.; Moszyński, D.; Guskos, N.; Ohtani, B.; Morawski, A. W. Preparation of photoactive nitrogen-doped rutile. *Appl. Surf. Sci.* **2013**, *266*, 410–419.

(12) Dolat, D.; Mozia, S.; Wróbel, R. J.; Moszyński, D.; Ohtani, B.; Guskos, N.; Morawski, A. W. Nitrogen-doped, metal-modified rutile titanium dioxide as photocatalysts for water remediation. *Appl. Catal., B* **2015**, *162*, 310–318.

(13) Kusiak-Nejman, E.; Wanag, A.; Kowalczyk, Ł.; Kapica-Kozar, J.; Colbeau-Justin, C.; Mendez Medrano, M. G.; Morawski, A. W. Graphene oxide-TiO₂ and reduced graphene oxide-TiO₂ nanocomposites: Insight in charge-carrier lifetime measurements. *Catal. Today* **2017**, *287*, 189–195.

(14) Sibera, D.; Narkiewicz, U.; Kapica, J.; Serafin, J.; Michalkiewicz, B.; Wróbel, R. J.; Morawski, A. W. Preparation and characterisation of carbon spheres for carbon dioxide capture. *J. Porous Mater.* **2019**, *26*, 19–27.

(15) Sibera, D.; Sreńscek-Nazzal, J.; Morawski, W. A.; Wróbel, B.; Serafin, J.; Wróbel, R. J.; Narkiewicz, U. Microporous carbon spheres modified with EDA used as carbon dioxide sorbents. *Adv. Mater. Lett.* **2018**, *9*, 432–435.

(16) Choma, J.; Kloske, M.; Dziura, A.; Stachurska, K.; Jaroniec, M. Preparation and Studies of Adsorption Properties of Microporous Carbon Spheres. *Eng. Prot. Environ.* **2016**, *19*, 169–182.

(17) Wickramaratne, N. P.; Jaroniec, M. Activated carbon spheres for CO₂ adsorption. *ACS Appl. Mater. Interfaces* **2013**, *5*, 1849–1855.

(18) Ludwinowicz, J.; Jaroniec, M. Potassium salt-assisted synthesis of highly microporous carbon spheres for CO₂ adsorption. *Carbon* **2015**, *82*, 297–303.

(19) Alcañiz-Monge, J.; Lozano-Castelló, D.; Cazorla-Amorós, D.; Linares-Solano, A. Fundamentals of methane adsorption in microporous carbons. *Microporous Mesoporous Mater.* **2009**, *124*, 110–116.

(20) Zheng, Y.; Li, Q.; Yuan, C.; Tao, Q.; Zhao, Y.; Zhang, G.; Liu, J.; Qi, G. Thermodynamic analysis of high-pressure methane adsorption on coal-based activated carbon. *Fuel* **2018**, *230*, 172–184.

(21) Policicchio, A.; MacCallini, E.; Agostino, R. G.; Ciuchi, F.; Aloise, A.; Giordano, G. Higher methane storage at low pressure and room temperature in new easily scalable large-scale production activated carbon for static and vehicular applications. *Fuel* **2013**, *104*, 813–821.

(22) Li, Y.; Qi, J.; Li, J.; Shen, J.; Liu, Y.; Sun, X.; Shen, J.; Han, W.; Wang, L. Nitrogen-Doped Hollow Mesoporous Carbon Spheres for

Efficient Water Desalination by Capacitive Deionization. *ACS Sustainable Chem. Eng.* **2017**, *5*, 6635–6644.

(23) Chen, A.; Li, Y.; Yu, Y.; Ren, S.; Wang, Y.; Xia, K.; Li, S. Nitrogen-doped hollow carbon spheres for supercapacitors application. *J. Alloys Compd.* **2016**, *688*, 878–884.

(24) Arif, A. F.; Kobayashi, Y.; Balgis, R.; Ogi, T.; Iwasaki, H.; Okuyama, K. Rapid microwave-assisted synthesis of nitrogen-functionalized hollow carbon spheres with high monodispersity. *Carbon* **2016**, *107*, 11–19.

(25) Wang, H.; Wang, W.; Xu, Y. Y.; Dong, S.; Xiao, J.; Wang, F.; Liu, H.; Xia, B. Y. Hollow Nitrogen-Doped Carbon Spheres with Fe₃O₄ Nanoparticles Encapsulated as a Highly Active Oxygen-Reduction Catalyst. *ACS Appl. Mater. Interfaces* **2017**, *9*, 10610–10617.

(26) Geng, H.; Zhou, Q.; Zheng, J.; Gu, H. Preparation of porous and hollow Fe₃O₄@C spheres as an efficient anode material for a high-performance Li-ion battery. *RSC Adv.* **2014**, *4*, 6430–6434.

(27) Sun, Y.; Wu, J.; Tian, J.; Jin, C.; Yang, R. Sulfur-doped carbon spheres as efficient metal-free electrocatalysts for oxygen reduction reaction. *Electrochim. Acta* **2015**, *178*, 806–812.

(28) Yin, B.; Wang, J.-t.; Xu, W.; Long, D.-h.; Qiao, W.-m.; Ling, L.-c. Preparation of TiO₂/mesoporous carbon composites and their photocatalytic performance for methyl orange degradation. *New Carbon Mater.* **2013**, *28*, 47–54.

(29) Orha, C.; Pode, R.; Manea, F.; Lazau, C.; Bandas, C. Titanium dioxide-modified activated carbon for advanced drinking water treatment. *Process Saf. Environ. Prot.* **2017**, *108*, 26–33.

(30) Kusiak-Nejman, E.; Wróbel, R. J.; Kapica-Kozar, J.; Wanag, A.; Szymańska, K.; Mijowska, E.; Morawski, A. W. Hybrid carbon-TiO₂ spheres: Investigation of structure, morphology and spectroscopic studies. *Appl. Surf. Sci.* **2019**, *469*, 684–690.

(31) Liu, J.; Qiao, S. Z.; Liu, H.; Chen, J.; Orpe, A.; Zhao, D.; Lu, G. Q. M. Extension of the stöber method to the preparation of monodisperse resorcinol-formaldehyde resin polymer and carbon spheres. *Angew. Chem., Int. Ed.* **2011**, *50*, 5947–5951.

(32) Asiltürk, M.; Şener, Ş. TiO₂ 2-activated carbon photocatalysts: Preparation, characterization and photocatalytic activities. *Chem. Eng. J.* **2012**, *180*, 354–363.

(33) Zhang, J.; Vasei, M.; Sang, Y.; Liu, H.; Claverie, J. P. TiO₂@Carbon Photocatalysts: The Effect of Carbon Thickness on Catalysis. *ACS Appl. Mater. Interfaces* **2016**, *8*, 1903–1912.

(34) Luttrell, T.; Halpegamage, S.; Tao, J.; Kramer, A.; Sutter, E.; Batzill, M. Why is anatase a better photocatalyst than rutile? - Model studies on epitaxial TiO₂films. *Sci. Rep.* **2015**, *4*, 4043.

(35) Pfeifer, V.; Erhart, P.; Li, S.; Rachut, K.; Morasch, J.; Brötz, J.; Reckers, P.; Mayer, T.; Rühle, S.; Zaban, A.; Mora Seró, I.; Bisquert, J.; Jaegermann, W.; Klein, A. Energy band alignment between anatase and rutile TiO₂. *J. Phys. Chem. Lett.* **2013**, *4*, 4182–4187.

(36) Pelech, I.; Pelech, R.; Kaczmarek, A.; Jędrzejewska, A.; Moszyński, D. Effect of treating method on the physicochemical properties of amine-functionalized carbon nanotubes. *Int. J. Mater. Res.* **2016**, *107*, 35–43.

(37) Thommes, M.; Kaneko, K.; Neimark, A. V.; Olivier, J. P.; Rodriguez-Reinoso, F.; Rouquerol, J.; Sing, K. S. W. Physisorption of gases, with special reference to the evaluation of surface area and pore size distribution (IUPAC Technical Report). *Pure Appl. Chem.* **2015**, *87*, 1051–1069.

(38) Hu, X.; Radosz, M.; Cychosz, K. A.; Thommes, M. CO₂-filling capacity and selectivity of carbon nanopores: Synthesis, texture, and pore-size distribution from quenched-solid density functional theory (QSDFT). *Environ. Sci. Technol.* **2011**, *45*, 7068–7074.

(39) Yin, G.; Liu, Z.; Liu, Q.; Wu, W. The role of different properties of activated carbon in CO₂ adsorption. *Chem. Eng. J.* **2013**, *230*, 133–140.

(40) Presser, V.; McDonough, J.; Yeon, S.-H.; Gogotsi, Y. Effect of pore size on carbon dioxide sorption by carbide derived carbon. *Energy Environ. Sci.* **2011**, *4*, 3059–3066.

(41) Kapica-Kozar, J.; Kusiak-Nejman, E.; Wanag, A.; Kowalczyk, Ł.; Wrobel, R. J.; Mozia, S.; Morawski, A. W. Alkali-treated titanium

dioxide as adsorbent for CO₂ capture from air. *Microporous Mesoporous Mater.* **2015**, *202*, 241–249.

(42) Michalkiewicz, B.; Majewska, J.; Kądziołka, G.; Bubacz, K.; Mozia, S.; Morawski, A. W. Reduction of CO₂ by adsorption and reaction on surface of TiO₂-nitrogen modified photocatalyst. *J. CO₂ Util.* **2014**, *5*, 47–52.

(43) Kapica-Kozar, J.; Piróg, E.; Wrobel, R. J.; Mozia, S.; Kusiak-Nejman, E.; Morawski, A. W.; Narkiewicz, U.; Michalkiewicz, B. TiO₂/titanate composite nanorod obtained from various alkali solutions as CO₂ sorbents from exhaust gases. *Microporous Mesoporous Mater.* **2016**, *231*, 117–127.

(44) Kapica-Kozar, J.; Michalkiewicz, B.; Wrobel, R. J.; Mozia, S.; Piróg, E.; Kusiak-Nejman, E.; Serafin, J.; Morawski, A. W.; Narkiewicz, U. Adsorption of carbon dioxide on TEPA-modified TiO₂/titanate composite nanorods. *New J. Chem.* **2017**, *41*, 7870–7885.